

$^{31}\text{P}(^3\text{He},p\gamma)^{33}\text{S}$ and $^{39}\text{K}(^3\text{He},p\gamma)^{41}\text{Ca}$ Reactions and the γ Decay of Analog States in ^{33}S and ^{41}Ca

K. T. Knöpfle, M. Rogge, and C. Mayer-Böricke

Max-Planck-Institut für Kernphysik, Heidelberg, Germany
and Institut für Kernphysik der Kernforschungsanlage Jülich, Jülich, Germany

and

D. S. Gemmell,* L. Meyer-Schützmeister, H. Ohnuma,† and N. G. Puttaswamy‡

Argonne National Laboratory, Argonne, Illinois 60439

(Received 31 December 1970)

Proton- γ -ray coincidence measurements have been made on the reactions $^{31}\text{P}(^3\text{He},p\gamma)^{33}\text{S}$ and $^{39}\text{K}(^3\text{He},p\gamma)^{41}\text{Ca}$ at incident ^3He energies of 12 and 13 MeV. The protons were detected at 0° to the beam direction, thereby preferentially selecting $L=0$ transfers of neutron-proton pairs. A Ge(Li) detector at 90° detected the γ rays with good energy resolution. Angular distributions for the $^{31}\text{P}(^3\text{He},p)^{33}\text{S}$ reaction were measured with a magnetic spectrograph. These, together with previous results on the $^{39}\text{K}(^3\text{He},p)^{41}\text{Ca}$ reaction, gave precise information on the intensities of the states excited, as well as their energies. The main purpose of the experiments was to measure the γ decay of the lowest-lying isobaric analog states in ^{33}S and ^{41}Ca . The analog state in ^{33}S was found to decay primarily (85%) to the 842-keV level and secondarily (15%) to the ground state. The analog state in ^{41}Ca decays in a more complex fashion to several states. The strongest transition (55%) is to the 4091-keV state. γ -ray decay schemes for several other low-lying even-parity levels in ^{33}S and ^{41}Ca were also measured. The observation that the 4091-keV level of ^{41}Ca decays (34%) to the $\frac{1}{2}^-$ ground state and (58%) to the $\frac{3}{2}^+$ level at 2009 keV suggests a $\frac{5}{2}^+$ assignment. The implications of the measurements are discussed, particularly with reference to the structure of low-lying two-particle-one-hole states in these nuclei.

I. INTRODUCTION

The study of the γ -ray decay properties of analog states is of interest because these states, while lying at excitation energies normally of several MeV, are expected to have relatively simple configurations. This is particularly so when the states are the isobaric analogs of the ground states of neighboring nuclei. The γ decay of such states to lower-lying levels gives valuable information about the (usually more complex) structure of these levels. The γ decay of analog states has been studied by several authors (as described, for example, in the review articles of Endt¹ and Hanna²). In the region of the upper s - d shell, Ern , Veltman, and Wintermans³ have studied the γ decay of negative-parity analog states, which are presumed to be formed by the coupling of a single $f_{7/2}$ nucleon to a core consisting of ^{32}S and some nucleons in the unfilled $1d_{3/2}$ shell. It was found that most of these analog states displayed a marked preference for decay to states having one unit less isospin, but having the same spin and parity as the emitting state.

In previous experiments, analog states in the region of the $2s$ - $1d$ shell have been mostly excited and studied via resonances in radiative-capture

reactions. In the work reported here, the γ decay of analog states that are bound (and thus not reachable in capture reactions) is studied by means of the ($^3\text{He},p\gamma$) reaction. In the simplest shell-model picture, the target nuclei ^{31}P and ^{39}K may be regarded as single-hole states in the $2s_{1/2}$ and $1d_{3/2}$ proton shells, respectively. The ^{33}S and ^{41}Ca states that are isobaric analogs of the ground states of ^{33}P and ^{41}K are therefore expected to be mainly of two-particle-one-hole nature. These states can be easily reached by means of the ($^3\text{He},p$) reaction on ^{31}P and ^{39}K and with the $L=0$ transfer of a $T=1$ neutron-proton pair. The angular distributions for such transfer are expected to peak strongly at 0° to the incident beam direction. Thus, in order to preferentially select these $L=0$ transfers, the proton detector in the present proton- γ coincidence measurement was placed at 0° . In order to sort out the γ -decay schemes, a high-resolution Ge(Li) γ -ray detector was used; and precise information on the energies and intensities of the states excited by the ($^3\text{He},p$) reaction was obtained from magnetic-spectrograph measurements.

In addition to the information on the analog states, the present experiments produced data on the γ decay of many other low-lying states in

^{33}S and ^{41}Ca . Most of the states populated strongly at 0° in the $(^3\text{He}, p)$ reaction are probably of positive parity and have predominantly a two-particle-one-hole structure. (For the $T_{\frac{1}{2}}$ states, both $T=0$ and $T=1$ neutron-proton pairs may contribute in the case of direct $L=0$ transfers.) Previously, little was known of the γ decay of these states, although they presumably have a relatively simple structure.

The present measurements on ^{31}P and ^{39}K targets complement previous $(^3\text{He}, p\gamma)$ measurements⁴ on an ^{27}Al target (which, in the simplest picture, has a ground state consisting of a single $1d_{5/2}$ hole).

II. EXPERIMENTAL ARRANGEMENT

The experiments were performed with ^3He beams of 12 and 13 MeV at the EN and MP tandem Van de Graaff accelerators of the Max-Planck-Institut (MPI) in Heidelberg and also at the FN tandem at the Argonne National Laboratory (ANL).

A. Proton Angular-Distribution Measurements

These measurements were performed at ANL with a split-pole magnetic spectrograph.⁵ The target was $45\text{-}\mu\text{g}/\text{cm}^2$ Zn_3P_2 on a $10\text{-}\mu\text{g}/\text{cm}^2$ carbon backing. The emergent protons were detected in nuclear emulsions, which were then developed and scanned by an automatic scanning machine.⁶ During the measurement, the photographic plates were covered with thin acetate foils to prevent scattered ^3He and other undesired particles from reaching the emulsion. The energy resolution obtained [~ 20 keV full width at half maximum (FWHM)] was adequate to study the groups of interest. An angular distribution was measured at nine angles in the range $7\text{--}49^\circ$. The region of excitation stud-

ied in ^{33}S by these means extended from $0\text{--}7.97$ MeV. A surface-barrier detector was used in the target chamber to monitor elastically scattered ^3He ions, and these data were then used to normalize the proton yields at the various angles.

B. Proton- γ Coincidence Measurements

These measurements were performed at both the MPI and the ANL with very similar experimental arrangements. Since the arrangement used at ANL has already been described in the literature,^{4,7} the description given here will be restricted to the system used at Heidelberg. Figure 1 shows a schematic diagram of the experimental setup. The incident ^3He beam was collimated by a series of tantalum apertures, which were shielded by a cylinder of lead around the beam line in order to minimize the background counting rate in the γ -ray detector.

The targets [$0.7\text{-mg}/\text{cm}^2$ Zn_3P_2 for the $^{31}\text{P}(^3\text{He}, p\gamma)$ reaction and $1.0\text{-mg}/\text{cm}^2$ KI (natural) for the $^{39}\text{K}(^3\text{He}, p\gamma)$ reaction] were evaporated onto gold backings $100\text{ }\mu\text{m}$ thick. The proton detector was either a lithium-drifted⁸ or an ion-implanted⁹ silicon counter with an active depth of $4\text{--}5$ mm (thick enough to stop 30-MeV protons). A $50\text{-}\mu\text{m}$ -thick gold foil was placed in front of this detector. The total thickness of gold ($150\text{ }\mu\text{m}$) was sufficient to stop the incident ^3He beam completely but allowed the high-energy protons from the $(^3\text{He}, p)$ reactions (whose Q values are 9.787 and 8.978 MeV for the targets ^{31}P and ^{39}K , respectively) to reach the silicon detector with relatively little energy loss. The contributions to the coincidence γ spectra from the other isotopes in the target (iodine, zinc, gold, and ^{41}K) were relatively very small and, because of the good energy resolution obtained in the γ spectra, were easily separated

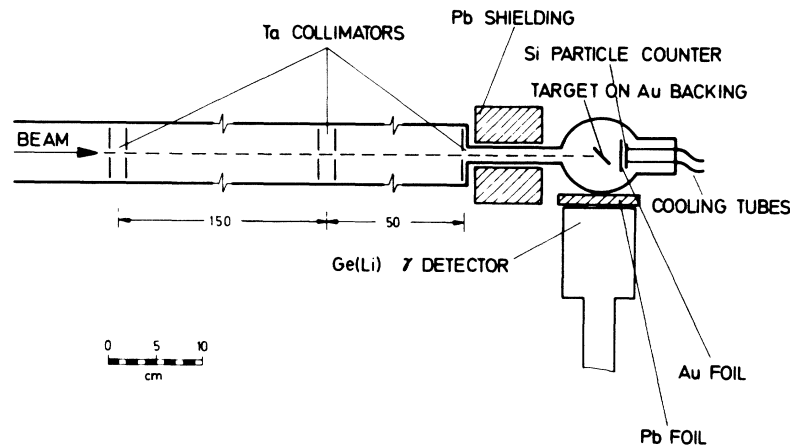


FIG. 1. Experimental arrangement with the target chamber, beam collimation and shielding, and the detectors for measuring coincident particles ($\sim 0^\circ$) and γ rays ($\sim 90^\circ$).

from the data sought on the ^{31}P and ^{39}K target isotopes. The proton detector was placed at 0° to the beam direction and subtended an angular range of $\pm 28^\circ$ at the target. When a lithium-drifted silicon detector was used, it was cooled by pumping liquid nitrogen through the copper support for the detector. The ion-implanted detector was cooled to -60°C by circulating methanol in a similar fashion. The resolution width for the detected protons varied from about 300–800 keV (depending on the energy) and was mainly determined by the energy loss and straggling of the incident ^3He beam in the target material. To minimize the number of detected “knock-on” protons from hydrogen impurities in the target, the chamber was kept below 10^{-6} Torr by means of a pump directly below the target.

The γ rays were detected by a 38.5-cc liquid-nitrogen-cooled Ge(Li) detector¹⁰ which could be positioned at angles in the range from 30 – 120° relative to the beam direction. The distance from the front face of the detector to the target was 6 cm. The total angle subtended at the target by the detector was 38° . Between the detector and the wall of the target chamber, 18 mm of lead were inserted to reduce the number of low-energy γ rays detected. This also served the purpose of providing a more favorable balance between the counting rates in the proton and γ -ray detectors.

The γ -ray detector gave a resolution width (FWHM) of 2 keV for the 1.17- and 1.33-MeV γ rays from a ^{60}Co source. In the $(^3\text{He}, p\gamma)$ coincidence measurements, the resolution obtained was somewhat worsened by Doppler shifts, by counting-rate problems, and by the energy dispersion (~ 2 keV per channel) available in the γ -ray spectra that were accumulated. The resolution (FWHM) obtained in these measurements was typically 6 keV for 2-MeV γ rays and 9 keV for 4-MeV γ rays.

Each laboratory measured the counting efficiency of its germanium detector as a function of γ energy. The measurements at MPI made use of a ^{56}Co source for γ -ray energies up to 3.5 MeV, and a Monte Carlo calculation (including the effect of the Pb in front of the detector) was used for the higher energies. For the ANL detector, calibrated γ -ray sources were used for energies up to 3.5 MeV, and use of the 0.992-MeV resonance in the $^{27}\text{Al}(p, \gamma)$ reaction extended the measurements up to $E_\gamma = 10.8$ MeV.

The γ -ray energy scale was calibrated against a ^{56}Co source which gives several γ rays between 800–3500 keV. A further calibration for both the particle and γ -ray energy scales was obtained by using known transitions in the reactions $^{12}\text{C}(^3\text{He}, p\gamma)^{14}\text{N}$ and $^{27}\text{Al}(^3\text{He}, p\gamma)^{29}\text{Si}$.

The principal experimental problems in the coincidence measurements stemmed from the low cross section for the $(^3\text{He}, p)$ reaction (typically about $100 \mu\text{b}/\text{sr}$ at $\theta_p = 0^\circ$) and from the low overall counting efficiency in both detectors. The low counting efficiency for the γ rays was an unavoidable property of the germanium detector. For the particle detector, a small solid angle was required in order to preferentially select those proton groups corresponding to $L = 0$ transitions. Thus, in order to achieve usable coincidence counting rates (~ 2 – 5 counts/sec) it was necessary to use relatively thick targets (~ 0.5 – 1.0 mg/cm²), beam currents of ~ 200 nA, and high singles counting rates in the detectors (as high as 30 000 counts/sec in the germanium detector). To maintain good γ -ray resolution at these high rates, considerable care was necessary in selecting and adjusting the

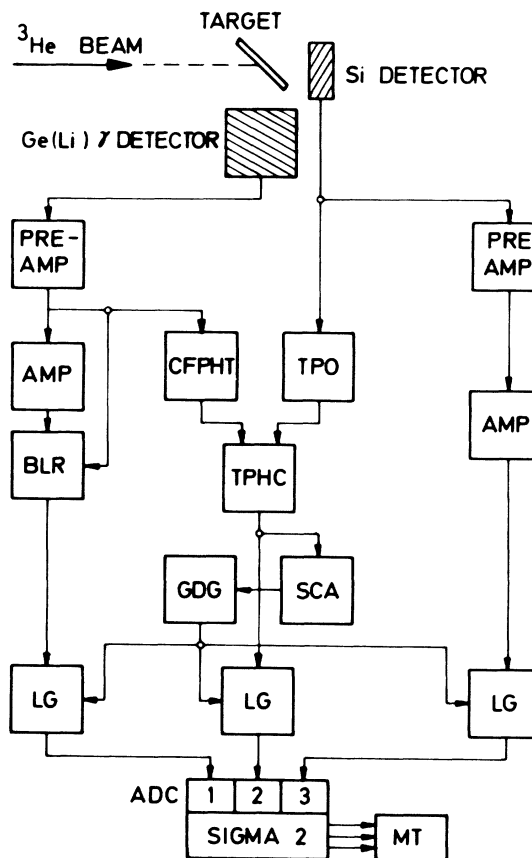


FIG. 2. Electronics for the three-parameter coincidence measurements at the MPI. This block diagram shows the connections of the preamplifiers, amplifiers, base-line restorer (BLR), constant-fraction pulse-height trigger (CFPHT), time pickoff (TPO), time-to-pulse-height converter (TPHC), gate and delay generator (GDG), single-channel analyzer (SCA), linear gates (LG), analog-to-digital converters (ADC), SIGMA-2 computer system, and magnetic tape (MT).

associated electronic circuitry.

Figure 2 shows a block diagram of the electronics used in the three-parameter measurement (of the γ -ray energy, the particle energy, and the time difference as measured with a time-to-pulse-height converter). The outputs were fed into the on-line SIGMA-2 computer system¹¹ at the MPI, and the digital coordinates for each event were stored on magnetic tape and could later be sorted either with the SIGMA-2 or an off-line CDC-3300 computer. The time resolution (FWHM) achieved with this was 16 nsec. By setting a window over a portion of the time spectrum that did not include the coincidence peak, it was possible to determine the contribution of random coincidences to the data. The γ -ray spectra were then corrected by subtraction of the random contribution. The 4096 channels used for the γ -ray spectra covered the γ -ray energy range from about 0–8 MeV; the particle energies and the time spectra were recorded in 1024 and 512 channels, respectively.

III. RESULTS

A. Measurements with Magnetic Spectrograph

The proton groups from the $^{31}\text{P}(^3\text{He}, p)^{33}\text{S}$ reaction were measured at laboratory angles of 7, 10, 13, 19, 25, 31, 37, 43, and 49° and for a bombarding energy $E(^3\text{He}) = 13$ MeV. The primary purposes of the measurements were (a) to establish the relative intensities of the various proton groups detected in the corresponding proton coincidence measurements, (b) to determine accu-

rately the energies of the levels thus populated in ^{33}S , and (c) to find out which transitions have angular distributions peaking strongly forward.

Figure 3 shows the proton spectrum obtained with the spectrograph at a laboratory angle of 7°. The proton groups are numbered and the corresponding excitation energies are listed in Table I. The excitation energies measured in this experiment, believed to be accurate to within ± 15 keV, are listed in column 2 of Table I. For comparison, the values given by Endt and Van der Leun¹² are given in column 3. At the higher excitation energies (above the first isobaric analog state), the level density becomes quite high; in this region therefore, only those levels seen in the present work are listed in column 3 of Table I. In the region of excitation energy below 5.5 MeV, the agreement between the level energies determined in this experiment and those given by Endt and Van der Leun is generally good (within 15 keV), although there is some evidence that the values measured here tend to become slightly higher than those given by Endt and Van der Leun as one goes to higher excitation energies. Above 5.5 MeV, the high-level density precludes a meaningful comparison.

Angular distributions were obtained for most of the levels listed in column 2 of Table I. In a few cases (including, unfortunately, a possible $T = \frac{3}{2}$ level at $E_{\text{exc}} = 7920$ keV), the proton groups were masked at some angles either by groups from impurities (indicated by an X in Fig. 3) or by strong neighboring proton groups. In Table I are listed the angles θ_{max} at which the angular

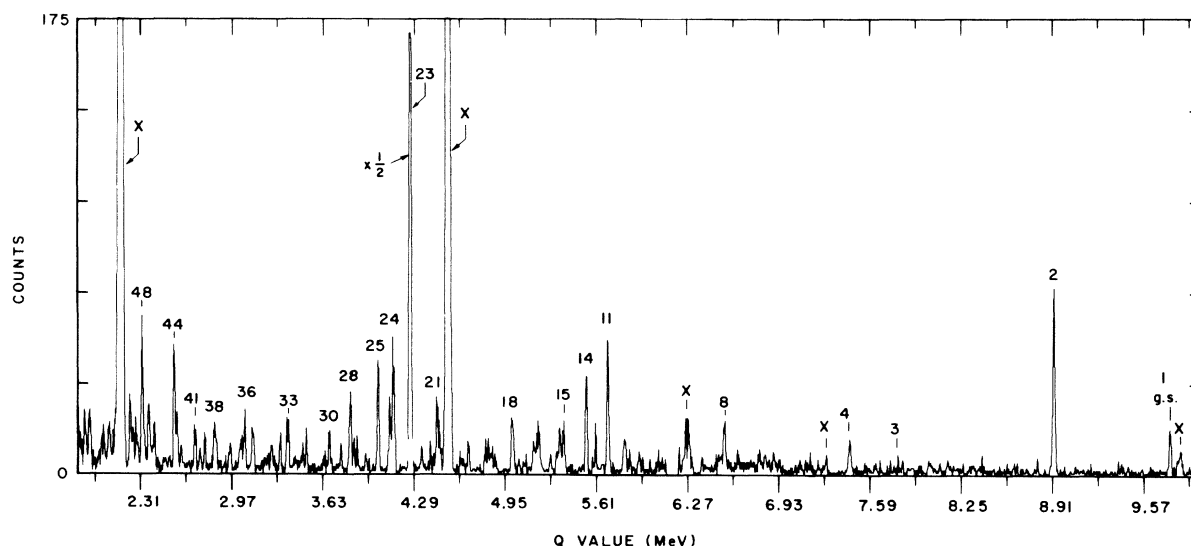


FIG. 3. Magnetic-spectrograph spectrum of protons from the $^{31}\text{P}(^3\text{He}, p)^{33}\text{S}$ reaction. The bombarding energy was 13 MeV and the spectrograph angle was 7°. The numbers refer to the positions of the observed levels in Table I. An X by a peak indicates that it is due to a contaminant.

TABLE I. Results for the $^{31}\text{P}(^3\text{He}, p)^{33}\text{S}$ reaction.

| Peak No. | Excitation energy | | θ_{\max} | Yield at θ_{\max} | J^π | l_n | | Section of Fig. 4 |
|----------|-------------------|------------|-----------------|--------------------------|----------------------------------|------------|---------------------------|-------------------|
| | Magnet (MeV) | Endt (keV) | | | | (d, p) | ($^3\text{He}, \alpha$) | |
| 1 | 0 | 0 | 15° | 35 | $\frac{3}{2}^+$ | 2 | | (c) |
| 2 | 843 | 842 | 7° | 110 | $\frac{1}{2}^+$ | 0 | 0 | (a) |
| 3 | 1967 | 1968 | | Weak | $\frac{5}{2}^{(+)}$ | (2) | | |
| 4 | 2315 | 2313 | 7° | 23 | $\frac{3}{2}^+$ | (2) | 2 | (a) |
| 5 | 2870 | 2869 | | Weak | | (2) | (2) | |
| 6 | 2938 | 2937 | 35° | 25 | $\frac{7}{2}^-$ | 3 | | (c) |
| 7 | 2973 | 2970 | 7° | 15 | | | | |
| 8 | 3220 | 3221 | 20° | 75 | $\frac{3}{2}^-$ | 1 | 1 | (b) |
| 9 | 3843 | 3832 | | Weak | | (3) | (3) | |
| 10 | 3947 | 3935 | Flat | 30 | | | | |
| 11 | 4068 | 4049 | 7° | 82 | | | | (a) |
| 12 | 4109 | 4095 | 10° | Weak | | | | |
| 13 | 4158 | 4145 | 10° | 25 | | | | |
| 14 | 4224 | 4213 | 12° | 75 | $\frac{3}{2}^-$ | 1 | | (b) |
| 15 | 4389 | 4377 | 7° | 29 | | | | (a) |
| 16 | 4439 | 4425 | 20° | 20 | | (4) | | |
| 17 | 4742 | 4732 | | Weak | | | | |
| 18 | 4761 | 4747 | 7° | 44 | | | | (a) |
| 19 | 4931 | 4920 | 14° | 26 | $(\frac{1}{2}, \frac{3}{2})^-$ | 1 | | |
| 20 | 4955 | 4941 | 23° | 26 | | | | |
| | | 5177 | | | $(\frac{5}{2}, \frac{7}{2})^-$ | (3) | (3) | |
| | | 5210 | | | | | | |
| 21 | 5294 | 5272 | Not resolved | | | | (2) | |
| | | 5287 | | | | | | |
| | | 5340 | | | | | | |
| | | 5351 | | | | | | |
| 22 | 5414 | 5399 | 15° | 23 | $(\frac{3}{2}, \frac{7}{2})^-$ | (3) | | |
| 23 | 5495 | 5479 | 7° | 560 | $\frac{1}{2}^+, T = \frac{3}{2}$ | | 0 | (a) |
| 24 | 5616 | | 7° | 86 | | | | |
| 25 | 5728 | | 15° | 85 | | | | (b) |
| 26 | 5882 | | | Weak | | | | |
| 27 | 5907 | | | Weak | | | | |
| 28 | 5931 | | 7° | 54 | | | | (a) |
| 29 | 5994 | | | Weak | | | | |
| 30 | 6083 | | | Weak | | | | |
| 31 | 6251 | | | Weak | | | | |
| 32 | 6278 | | | Weak | | | | |
| 33 | 6384 | | 20° | 60 | | | (2) | (b) |

TABLE I (Continued)

| Peak No. | Excitation energy | | θ_{max} | Yield at θ_{max} | J^π | l_n (d, p) | l_n ($^3\text{He}, \alpha$) | Section of Fig. 4 |
|----------|-------------------|------------|-----------------------|--------------------------------|------------------------------------|------------------|---------------------------------|-------------------|
| | Magnet (MeV) | Endt (keV) | | | | | | |
| 34 | 6438 | | | | | | | |
| 35 | 6635 | | 7° | 33 | | | | |
| 36 | 6697 | | 20° | 55 | | | | (b) |
| 37 | 6802 | | 10° | 27 | | | | |
| 38 | 6912 | | 25° | 50 | | | | |
| 39 | 6983 | | 20° | 65 | $\frac{3}{2}^+, T = \frac{3}{2}$ | (2) | (6900) | (b) |
| 40 | 7018 | | | Weak | | | | |
| 41 | 7052 | | 7° | 30 | | | | |
| 42 | 7153 | | Weak | | | | | |
| 43 | 7183 | | 22° | 60 | | | | (b) |
| 44 | 7206 | | 14° | 90 | | | | (a) |
| 45 | 7351 | | 10° | 44 | | | | |
| 46 | 7383 | | 10° | 62 | | | | |
| 47 | 7415 | | 30° | 30 | | | | |
| 48 | 7435 | | 7° | 85 | | | | (a) |
| 49 | 7473 | | 23° | 56 | $\frac{3}{2}^+, T = \frac{3}{2}$ | (3) | (7348) | (b) |
| 50 | 7498 | | Flat | 34 | | | | |
| 51 | 7521 | | 7° | 46 | | | | |
| 52 | 7580 | | Contaminant obscures | | | | | |
| 53 | 7613 | | | Weak | | | | |
| 54 | 7679 | | | Weak | | | | |
| 55 | 7713 | | | Weak | | | | |
| 56 | 7830 | | 14° | 43 | | | | |
| 57 | 7860 | | | Weak | | | | |
| 58 | 7920 | | | (Strong) | $(\frac{3}{2}^+, T = \frac{3}{2})$ | | | |

distributions reach a maximum and also the relative yields measured at those angles. Some of these angular distributions are plotted in Fig. 4, and column 9 of Table I indicates the section in which they are displayed.

In Fig. 4, the various angular distributions have been sorted into groups that exhibit similar characteristics. For example, there are several distributions that peak strongly toward 0°, suggesting an $L=0$ deuteron transfer. Among the more intense transitions in this group are those populating the 842-keV first excited state and the 5479-keV isobaric analog state (both of which have spin and parity $\frac{1}{2}^+$).

From measurements at those angles at which contaminants do not interfere, it is evident that the transition to the state at $E_{\text{exc}} = 7920$ keV is a

strong one. The data are, however, insufficient to establish the shape of the angular distribution.

The angular distributions of protons from the $^{31}\text{P}(^3\text{He}, p)^{33}\text{S}$ reaction has been measured previously by Cox, West, and Ascutto,¹³ who used a bombarding energy of 6 MeV and detected the protons with semiconductor counters. Their angular distributions are frequently very different in shape from those measured here (e.g., their distribution for the ground-state group is peaked very strongly forward). These differences are perhaps attributable to their lower bombarding energy.

B. Proton- γ -Ray Coincidence Measurements

1. $^{31}\text{P}(^3\text{He}, p\gamma)^{33}\text{S}$ Reaction

Figure 5(a) shows the singles particle spectrum and Fig. 5(b) shows the particle spectrum obtained

in coincidence with all γ rays detected in the γ -ray counter. For comparison, Fig. 5(c) also gives the intensities and positions of the various proton groups that were found on the basis of the high-resolution measurements with the magnetic spectrograph. The intensities shown in Fig. 5(c) were determined by integrating the angular distributions measured with the spectrograph over the solid-angle region subtended by the proton detector in the coincidence measurements. As the data in Fig. 5 indicate, the transition to the state in ^{33}S at $E_{\text{exc}} = 5479$ keV (the isobaric analog of the ground state of ^{33}P) is relatively intense. The large peak near channel 300 in Fig. 5(a) is due to deuterons feeding the ground state of ^{32}S in the $^{31}\text{P}(^3\text{He}, d)^{32}\text{S}$ reaction. In the coincidence spectrum [Fig. 5(b)], the peaks seen in the channels below about channel 400 contain large contributions from the $^{12}\text{C}(^3\text{He}, p\gamma)^{14}\text{N}$ and the $^{31}\text{P}(^3\text{He}, d\gamma)^{32}\text{S}$ reactions in addition to that from the $^{31}\text{P}(^3\text{He}, p\gamma)^{33}\text{S}$ reaction.

The experimental data were analyzed and the γ -decay schemes for the levels excited were determined by obtaining (from the data recorded on magnetic tape) the γ -ray spectra in coincidence with various regions of the particle spectrum. Usually about 200 adjacent windows, each five channels wide, were set over the particle spectrum. The corresponding 200 γ -ray spectra were accumulated from tape and then stored for use in further analysis. The spectra were added together in different combinations to determine the γ -decay

schemes of the states involved. In this fashion it was possible to sort out the γ rays from the various initial states, even though the individual states were frequently not resolved from one another in the proton spectrum. In sorting out the γ decays, it was very helpful to have the information from the spectrograph measurement. This supplied highly accurate energies and intensities of the levels expected in the proton spectrum from the solid-state counter. This information, coupled with the good energy resolution of the γ -ray detector, was sufficient in nearly all cases to unambiguously identify a measured γ -ray energy with an energy difference between two known levels in ^{33}S .

Figure 6 shows the γ -ray spectrum obtained in coincidence with protons leading to the analog state at 5.48 MeV (corresponding to proton channels 475–495 in Fig. 5). The analog state decays predominantly [(85 \pm 5)%] to the first excited state at 0.842 MeV and also to the ground state [(15 \pm 5)%]. These branching ratios are determined both from the photopeaks and from the double-escape peaks, and are based on the assumption that the primary γ rays have an isotropic angular distribution (the spin of the analog state is presumed to be $\frac{1}{2}^+$).

The γ -decay schemes of several other levels in ^{33}S were also extracted from the data. For these, however, the statistical accuracy was mostly insufficient to permit the determination of useful values for the branching ratios.

The γ -decay schemes measured in these experi-

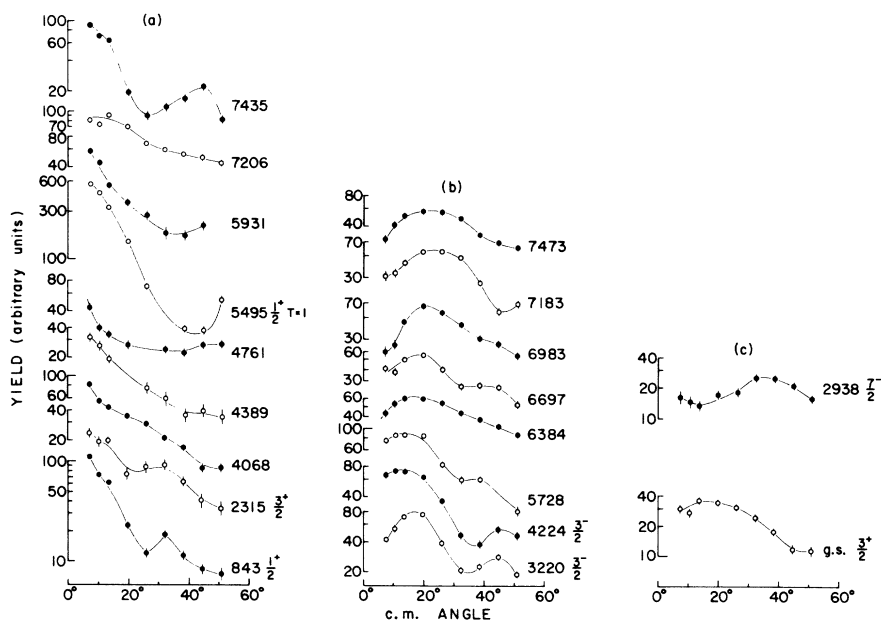


FIG. 4. (a)–(c) Some angular distributions for the $^{31}\text{P}(^3\text{He}, p)^{33}\text{S}$ reaction, as measured with the magnetic spectrograph. The excitation energies of the levels in ^{33}S are listed with the distributions.

ments, together with those previously known¹² in ^{33}S , are shown in Fig. 7. Figure 7 also illustrates the intensities [Fig. 5(c)] expected in the proton detector for the various groups populating levels in ^{33}S . As indicated in the figure, the present experiments determine many previously unknown

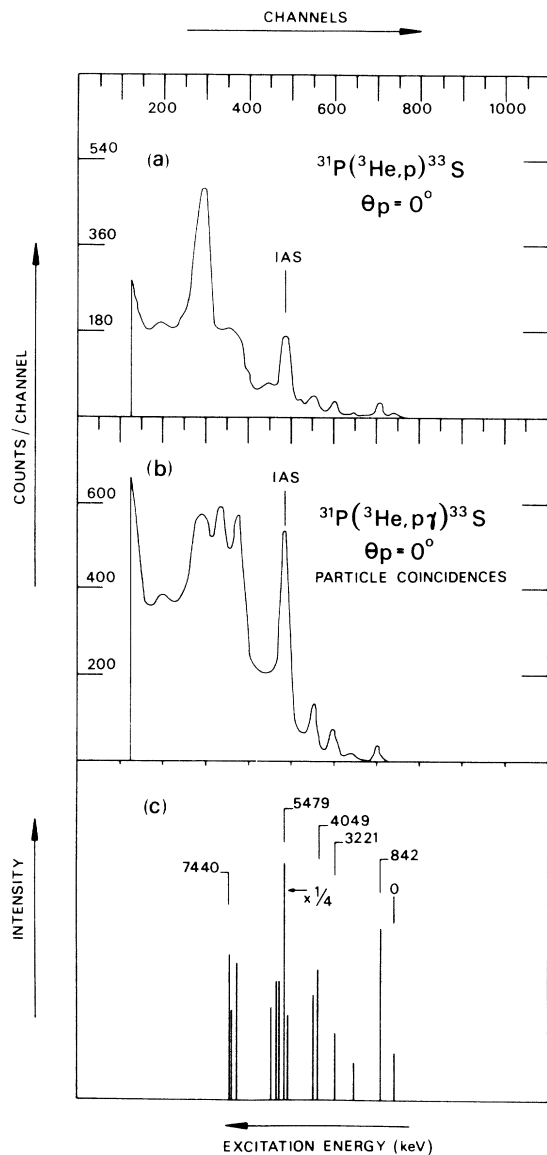


FIG. 5. Particle spectra obtained for the $^{31}\text{P}(^3\text{He}, p)^{33}\text{S}$ reaction. (a) Singles spectrum; i.e., all particles detected at 0° by use of the arrangement shown in Fig. 1. (b) Particle spectrum obtained in coincidence with detected γ rays of all energies. (c) Position intensities expected for the various proton groups on the basis of the magnetic-spectrograph measurements. To obtain these data, which are plotted on the same energy scale as (a) and (b), the spectrograph data were integrated over the solid angle subtended at the target by the particle detector. The numbers refer to excitation energies of levels in ^{33}S .

γ -decay schemes in ^{33}S . The γ decays determined by the present measurements are drawn in on the right-hand side of Fig. 7, while those previously known and given in Ref. 12 are shown on the left-hand side. The filled circles in Fig. 7 designate the starting points of γ transitions whose existence is quite definite. The open circles indicate transitions which are either weak (<5%) or uncertain. The levels whose decay schemes are determined for the first time by the present measurements are those at excitation energies of 2970, 3832, 3935, 4049, 4213, 4377, 4747, 6091, 6380, and 7930 keV in ^{33}S . The level at 4213 keV is seen here to decay predominantly to the level at 2869 keV. Previously,¹² the main transition from this level was thought to be to the first excited state.

An earlier measurement¹⁴ of the γ -decay properties of the 5479-keV analog state via the $^{34}\text{S}(^3\text{He}, \alpha\gamma)^{33}\text{S}$ reaction led to the determination of a 15% γ -ray branch to a level at 2950-keV excitation energy. As the γ spectrum (Fig. 6) shows, the present experiments give no indication of the existence of this transition.

The excitation energy of the first isobaric analog state in ^{33}S has been previously determined as 5479 ± 6 keV¹² and 5479 ± 15 keV.¹⁴ The present magnetic-spectrograph measurements give 5495 ± 15 keV. However, perhaps the most accurate estimate of this energy is given by the present measurements with the Ge(Li) γ -ray detector, from which the energy of the ground-state γ ray was determined to be 5475.0 ± 1.6 keV. The sum of the energies of the transitions between the analog and the first excited state and between the first excited state and the ground state was measured as $4632.7 \pm 1.0 + 841.8 \pm 1.0 = 5474.5 \pm 1.4$ keV.

2. $^{39}\text{K}(^3\text{He}, p\gamma)^{41}\text{Ca}$ Reaction

For the $(^3\text{He}, p\gamma)$ reaction on ^{39}K , Fig. 8 shows (a) the single-particle spectrum, (b) the particle spectrum in coincidence with all γ rays, and, for comparison, (c) the intensities and energies of the various proton groups that are expected (after integrating over the solid angle of the present proton detector) on the basis of the magnetic-spectrograph measurements of Belote *et al.*¹⁵ The analysis of the coincidence data for the $^{39}\text{K}(^3\text{He}, p\gamma)^{41}\text{Ca}$ reaction proceeded in a fashion similar to that already described for the $^{31}\text{P}(^3\text{He}, p\gamma)^{33}\text{S}$ reaction.

Figures 9–11 show the γ -ray spectra measured in coincidence with various proton windows set to cover some of the regions of interest in the particle spectrum (Fig. 8). The corresponding channels in the particle spectrum are given in the figure captions together with the energies and par-

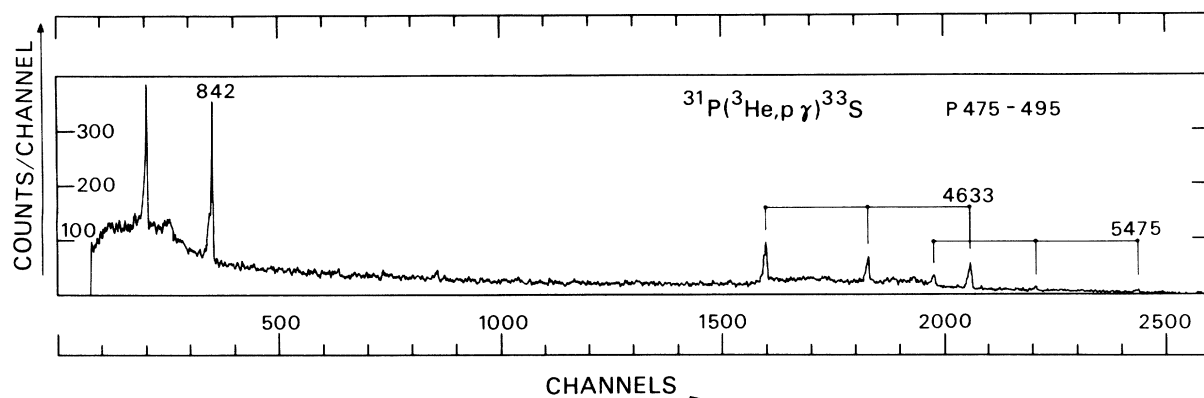


FIG. 6. γ -ray spectrum obtained for the $^{31}\text{P}(^3\text{He},p\gamma)^{33}\text{S}$ reaction, showing the γ decay of the lowest isobaric analog state at 5475 keV in ^{33}S . (This spectrum is obtained in coincidence with protons whose energies fall within channels 475–495 in Fig. 5.) The energy of each high-energy γ ray is given, and the positions of its photopeak and its single- and double-escape peaks are marked. The analog state decays to the 842-keV level (85%) and to the ground state (15%).

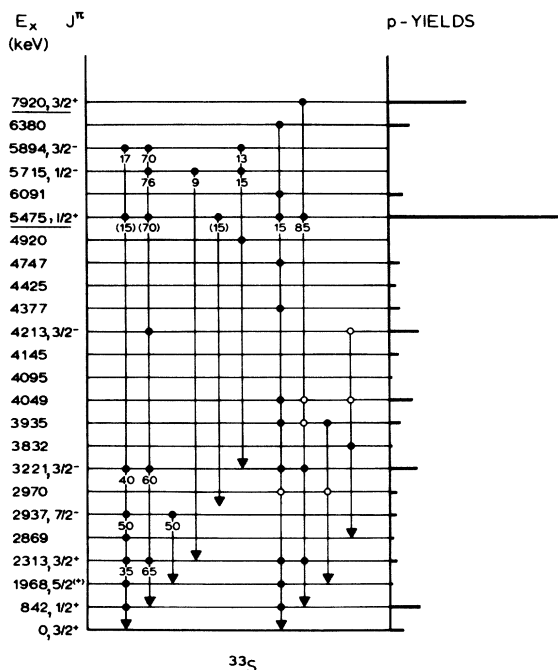


FIG. 7. γ -ray decay scheme for ^{33}S . The excitation energies and spins and parities are those given in Ref. 12 with the exception of the two analog states (underlined) and of the 6091-keV level. In these three cases, the energies given are those determined in the present work. The convention used here is that each closed circle represents the origin of a γ transition. All transitions to any one level are represented on one vertical line. On the left-hand side of the figure are drawn previously known (Ref. 12) transitions and on the right-hand side are the γ decays measured in the present work. (Note: Not all known levels are included. For the sake of clarity, only the levels whose γ decay is known are shown here.) An open circle indicates that the γ decay involved is weak or uncertain. The horizontal lines on the right-hand side have lengths proportional to the yields [Fig. 5(c)] near 0° for proton groups from the $^{31}\text{P}(^3\text{He},p)^{33}\text{S}$ reaction.

icipating levels for the dominant γ rays seen in the spectra.

From many such γ -ray spectra (and by no means only from those shown in Figs. 9–11), γ -ray decay schemes (many of them not previously known) were determined for several levels in ^{41}Ca . Figure 12 shows the decay schemes previously known¹² and also those measured in the present work. The conventions used in Fig. 12 are the same as were used in Fig. 7. Also shown are the relative intensities [Fig. 8(c)] of the detected proton groups as determined from the magnetic spectrograph measurements of Belote *et al.*¹⁵

In the γ -ray spectra measured for the $^{39}\text{K}(^3\text{He},p\gamma)^{41}\text{Ca}$ reaction, the statistical accuracy was generally better than that in the spectra measured for the $^{31}\text{P}(^3\text{He},p\gamma)^{33}\text{S}$ reaction. (This was, in fact, necessary because, in contrast to the decay in ^{33}S , the γ decay of the analog state in ^{41}Ca is split into many components.) As a consequence, it was possible to determine branching ratios for many of the γ -ray decay schemes measured in this work. Again, it was assumed that the γ rays were emitted isotropically. For the states formed by $L=0$ deuteron transfer – and it is supposed that most of the intense states seen in these measurements are of this type – this assumption is certainly valid. For other values of the transferred L , or for spins greater than $\frac{1}{2}$, the primary γ rays may not be isotropic, and thus the branching ratios calculated on the basis of isotropy may be in error. The magnitude of such an error is hard to estimate; despite this uncertainty, the branching ratios measured at $\theta_\gamma = 90^\circ$ are given here because they do convey useful information.

In Fig. 12, two sets of level energies are given: firstly, those that could be determined from the energies of the γ rays seen in the present experi-

ments and, secondly, the level energies given in Tables 41.7 and 41.8 of Ref. 12 and by Johnson *et al.*¹⁶ The systematic error of the γ -energy calibration of the present work is estimated to be ≤ 2 keV; the relative errors of the individual level energies are quoted below. In most cases, the

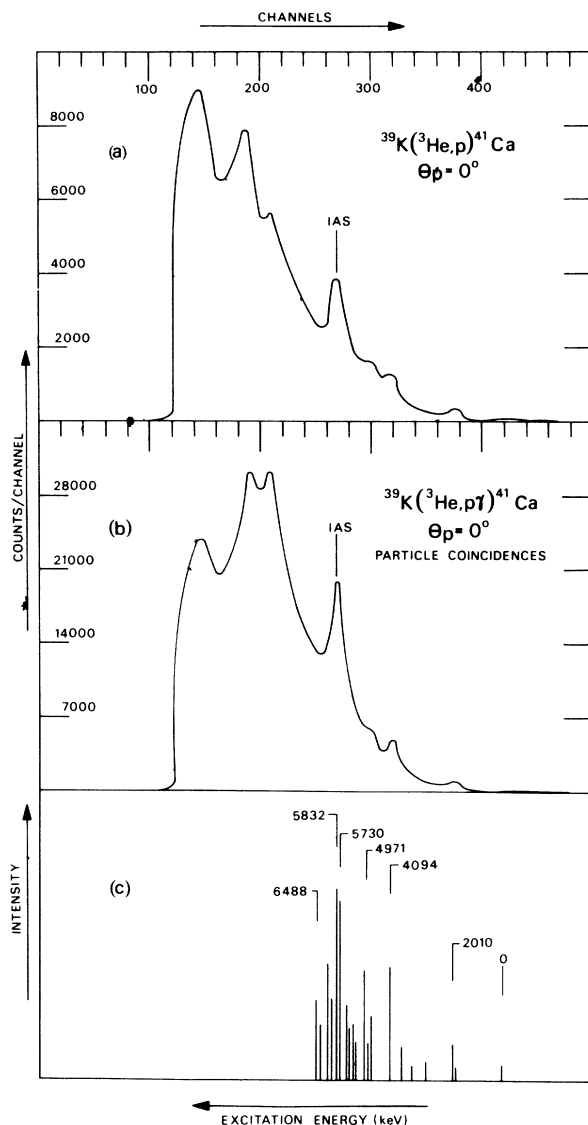


FIG. 8. Particle spectra obtained for the $^{39}\text{K}(^3\text{He}, p)^{41}\text{Ca}$ reaction. (a) Singles spectrum, i.e., all particles detected at 0° by use of the arrangement shown in Fig. 1. (b) Particle spectrum obtained in coincidence with detected γ rays of all energies. (c) Intensities expected for the various proton groups on the basis of the magnetic-spectrograph measurements of Ref. 15. To obtain these data, which are plotted on the same energy scale as (a) and (b), the spectrograph data were integrated over the solid angle subtended at the target by the particle detector. The numbers refer to excitation energies of levels in ^{39}K .

agreement between the two sets of energies below 5-MeV excitation energy is good. In the energy region above 5.25 MeV, the level energies determined in the present work are systematically ~ 15 keV lower than the values given in Ref. 12. This is most likely due to the fact that Endt and Van der Leun¹² used a systematic difference between the excitation energies given by Belote *et al.*¹⁵ and some more precise energy values determined by Gruppelaar and Spilling¹⁷ to correct the former values at excitation energies below 5 MeV, but did not apply this correction above 5 MeV.

Some of the γ rays observed are listed in the captions for Figs. 9–11 and also indicated in Fig. 12. In the following we summarize the energies and branching ratios of the transitions observed, and include some explanatory comments where appropriate. (The energies given are those determined in the present work.)

The previously known^{12, 16} ground-state transitions from the levels at 1942.0 ± 0.6 , 2009.2 ± 0.5 , 2574.4 ± 2.0 , 2603.8 ± 1.0 , 2880.5 ± 2.0 , and 3199.4 ± 1.0 keV were also observed here. The γ ray from the 2881-keV level was found to be broader than normal, either because an unresolved doublet was being observed or because the level has a lifetime long enough to produce a substantial Doppler broadening. The previously known decay of the 3398.4 ± 1.0 -keV level to the level at 2009 keV was also observed.

The 3738.0 ± 1.0 -keV level decays to the 2009-keV (60%) and 2604-keV (40%) levels. There is no indication in the present work of a ground-state branch from this level, although such a branch has been reported previously.¹⁶

The 4091.4 ± 1.0 -keV level decays mainly to the ground state (34%) and to the 2009-keV level (58%). A weak branch ($\sim 8\%$) goes also to the 2604-keV; and possibly there is also a transition of comparable intensity to the 2881-keV level, although this is not certain.

The 4180.0 ± 1.0 -keV level decays to the 2009-keV (70%) and 2604-keV (30%) levels. (Johnson *et al.*¹⁶ measured relative intensities of 50% and 50% from this level, and were unable to determine the exact levels to which the transitions proceeded.)

The 4723.9 ± 1.0 -keV level was observed to decay to the ground state (10%) and to the 2009-keV level (90%). A possible weak branch to a level at 3495 keV could not be verified.

The 4768.4 ± 1.0 -keV level appeared to be fed from a higher level (possibly the 4961-keV level). The experimental excitation energy of this level provides the only case in which the difference between the present value and that of Ref. 12 is larger than could be expected from the errors. The 4768-keV level decays 100% to the 2009-keV

level.

The decay of the 4811.0 ± 2 -keV level was difficult to sort out. The strongest transition is certainly to the ground state. There is a fairly strong transition to the 1942-keV level, but a branching ratio could not be established because the γ -ray energy (2869 keV) lies too close to that of the transition from the 2881-keV state (which, as mentioned above, gives rise to an abnormally broad peak in the spectrum). A transition to the 2881-keV level is also a possibility that cannot be ruled out by the data. A weak transition to the 2009-keV level exists.

The 4876 ± 3 -keV level, known¹² to be a negative-parity state [since it is an $l_n = 3$ transition in the (d, p) reaction], decays predominantly to the ground state. It was not possible to determine whether this level was fed by γ transitions from higher states or whether it was itself weakly excited in the ($^3\text{He}, p$) reaction.

The 4961 ± 4 -keV level decays to the ground state (65%) and to the 2881-keV level (35%). There is also a possibility that a γ decay from this state feeds the 4768-keV level.

The decay of the levels at 5111 ± 5 and 5284 ± 5 keV could not be determined uniquely. The one certain transition here was that from the 5284-keV to the 2009-keV level.

The 5411.5 ± 2 -keV level decays strongly (63%) to the 1942-keV level [in our measurements transitions to this level ($\frac{3}{2}^-$) were rarely observed] and also (37%) to the 2604-keV level. The data also suggested weak transitions to the levels at 2463 and 2957 keV, but these were uncertain.

The 5470 ± 4 -keV level decays strongly to the ground state, but the measurement of its relative intensity was rendered difficult because of the fact that the single- and double-escape peaks for this γ ray almost coincide with peaks due to the 4961-keV γ ray.

The 5716.2 ± 2 -keV level decays to the ground state (25%) and to the 2009-keV (55%) and 4180-keV (20%) levels. A possible weak transition to the 1942-keV level could not be substantiated.

The first isobaric analog state, whose energy was measured to be 5812.7 ± 1 keV, decays to the 3398-keV (25%), 3738-keV (20%), and 4091-keV (55%) levels. The upper intensity limit for a possible weak branch to the level at 2009 keV is <5%; however, the spectra offer no real evidence for the existence of this transition.

The 5972 ± 2 -keV level decays to the levels at 2009, 2578, 2604, and 3398 keV with roughly equal probability.

The 6323 ± 4 -keV level decays predominantly to the first excited state at 1942 keV.

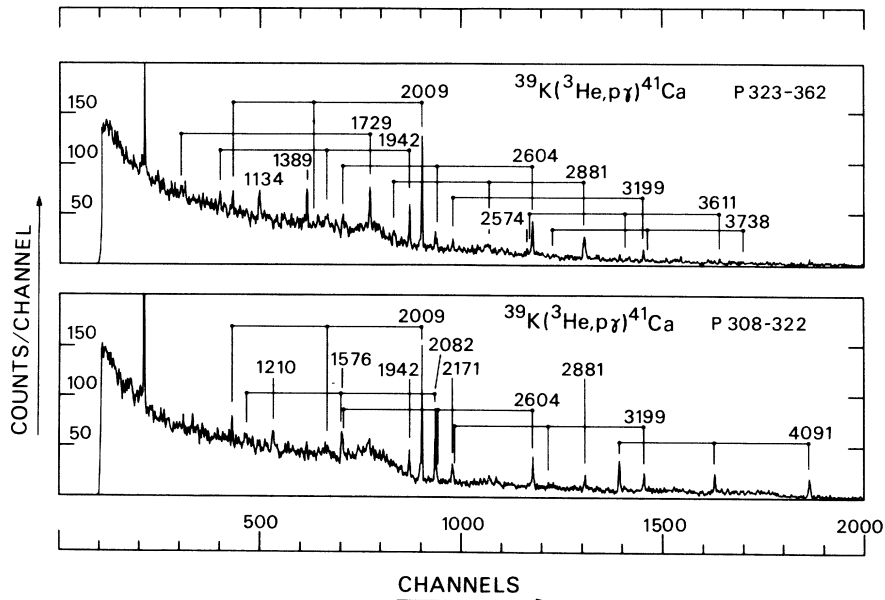


FIG. 9. Spectra showing the γ rays measured in coincidence with proton groups emerging in the particle spectrum for the reaction $^{39}\text{K}(^3\text{He}, p)^{41}\text{Ca}$ (Fig. 8) in channels 323–362 (upper spectrum) and 308–322 (lower spectrum). For some of the γ transitions, the energy of the photopeak is given and also (where existing) the positions of their single- and double-escape peaks. The energies (keV) of each transition and of its initial and final states in ^{41}Ca , given in the form $E_\gamma = E_x^i - E_x^f$, are 1134 = 3738 – 2604, 1210 = 4091 – 2881, 1389 = 3398 – 2009, 1576 = 4180 – 2604, 1729 = 3738 – 2009, 1942 = 1942 – g.s., 2009 = 2009 – g.s., 2082 = 4091 – 2009, 2171 = 4180 – 2009, 2574 = 2574 – g.s., 2604 = 2604 – g.s., 2881 = 2881 – g.s., 3199 = 3199 – g.s., (3611 = 3611 – g.s.), (3738 = 3738 – g.s.), 4091 = 4091 – g.s.

The 6091- and 6488-keV levels, although strongly excited in the $^{39}\text{K}(^3\text{He}, p)^{41}\text{Ca}$ reaction at $\theta_p = 0^\circ$, showed no dominant γ -ray decay modes in these measurements.

The γ decay of the second isobaric analog state (expected at about $E_{\text{exc}} = 6.8$ MeV) could not be determined in these measurements. It is possible that this state, which one would expect to be excited in the $(^3\text{He}, p)$ reaction at forward angles, decays principally by α -particle emission – even though such decay is forbidden by isospin selection rules and inhibited by considerations of angular momentum.

IV. DISCUSSION

It is of interest to compare the γ -ray decay schemes measured here for the lowest isobaric analog states in ^{33}S and ^{41}Ca with other measurements in this mass region. Several instances have been found in which isobaric analog states exhibit a strong preference for an $M1$ γ decay to lower-lying states having an isobaric spin one unit less than that of the emitting state, but having the same spin and parity. These “peculiar” γ decays were first noticed by Ern e *et al.*³ and have since been summarized and discussed by several authors (e.g., Maripuu,¹⁸ Kurath,¹⁹ and contributors to Refs. 1 and 2). It is now commonly accept-

ed that these strong $M1$ transitions occur between states having the same spin and spatial configurations but differing in their isospin coupling.

For the cases of ^{33}S and ^{41}Ca , there is evidence (to be discussed below) that the $T_<$ states corresponding to the lowest isobaric analog states lie at 842 keV in ^{33}S and at 2010 keV in ^{41}Ca . Thus the present measurements confirm the expected strong γ decay from the 5479-keV ($\frac{1}{2}^+$, $T = \frac{3}{2}$) level to the 842-keV ($\frac{1}{2}^+$, $T = \frac{1}{2}$) level in ^{33}S , but the expected decay from the 5832-keV ($\frac{3}{2}^+$, $T = \frac{3}{2}$) level to the 2010-keV ($\frac{3}{2}^+$, $T = \frac{1}{2}$) in ^{41}Ca was not observed. It is furthermore interesting to note that in ^{33}S (which one would expect to be a complicated nucleus from the shell-model point of view) the γ -decay scheme of the analog state is quite simple, whereas in ^{41}Ca (which one might expect to be a somewhat more simple nucleus) the analog state decays in a complicated fashion via several different branches.

In addition to giving precise values for the intensities and energies of proton groups expected in the coincidence experiments, the magnetic-spectrograph measurements reported here for $^{31}\text{P}(^3\text{He}, p)^{33}\text{S}$ and by Belote *et al.*¹⁵ for $^{39}\text{K}(^3\text{He}, p)^{41}\text{Ca}$ yield information on the structure of the states whose γ decay is being studied. In a simplified shell-model description, one would picture the ground states of the target nuclei ^{31}P and ^{39}K

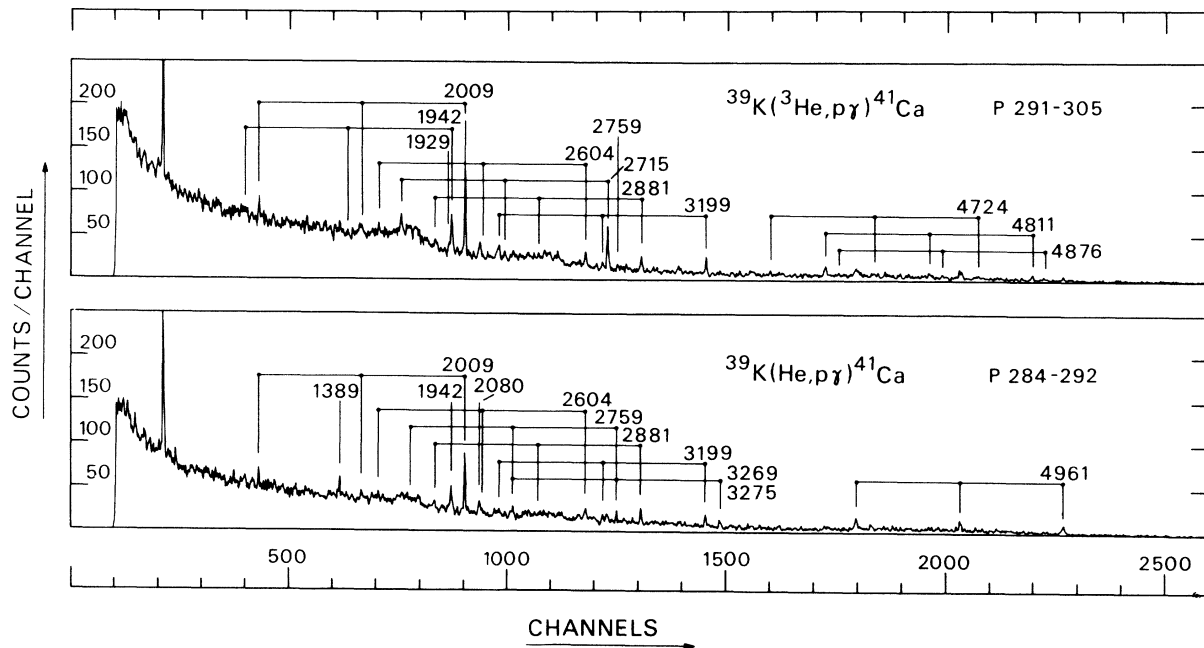


FIG. 10. Coincidence spectra as in Fig. 9, except that the ranges of channel numbers are 291–305 (upper spectrum) and 284–292 (lower spectrum). The energies $E_\gamma = E_x^i - E_x^f$ (keV) for the peaks are 1389 = 3398 – 2009, 1929 = 4811 – 2881, 1942 = 1942 – g.s., 2009 = 2009 – g.s., 2080 = 4961 – 2881, 2604 = 2604 – g.s., 2715 = 4724 – 2009, 2759 = 4768 – 2009, 2881 = 2881 – g.s., 3199 = 3199 – g.s., 3269 = 5211 – 1942, 3275 = 5284 – 2009, 4724 = 4724 – g.s., 4811 = 4811 – g.s., 4876 = 4876 – g.s., 4961 = 4961 – g.s.

as being single holes in the $2s_{1/2}$ and $1d_{3/2}$ shells, respectively. Then one would expect that the direct transfer of an $L=0$ neutron-proton pair by means of the (${}^3\text{He}, p$) reaction on these nuclei would preferentially populate those states in ${}^{33}\text{S}$ and ${}^{41}\text{Ca}$ that have two-particle-one-hole configurations.

Among the angular distributions measured for ${}^{31}\text{P}({}^3\text{He}, p){}^{33}\text{S}$, there are a few that peak strongly forward and thus suggest an $L=0$ transfer. By far the most intense of these are the ones for those proton groups leaving ${}^{33}\text{S}$ in its analog state at 5479 keV and in its first excited state at 842 keV. Thus, one might anticipate that the main shell-model configurations contributing to these states would be

$$[s_{1/2}^3(\frac{1}{2}, \frac{1}{2})d_{3/2}^2(0, 1)]_{(1/2, 3/2)}$$

and

$$[s_{1/2}^3(\frac{1}{2}, \frac{1}{2})d_{3/2}^2(0, 1)]_{(1/2, 1/2)},$$

respectively. Here an inert core of ${}^{28}\text{Si}$ is assumed and the numbers in parentheses are the spin and isospin couplings for the three nucleons in the $2s_{1/2}$ shell and the two nucleons in the $1d_{3/2}$ shell. For the 842-keV level, the configuration $[s_{1/2}^3(\frac{1}{2}, \frac{1}{2})d_{3/2}^2(1, 0)]_{(1/2, 1/2)}$ can also contribute. [In ${}^{34}\text{Cl}$, the $d_{3/2}^2(1, 0)$ configuration has recently

been measured²⁰ to lie 0.67 MeV above the $d_{3/2}^2(0, 1)$ configuration.] The idea that the 842- and 5479-keV levels contain principally the configurations $s_{1/2}^3d_{3/2}^2(0, 1)$ is supported by evidence from other particle-transfer reactions [e.g., measurements¹⁴ on the ${}^{34}\text{S}({}^3\text{He}, \alpha){}^{33}\text{S}$ reaction] and also by the calculations of Glaudemans *et al.*²¹⁻²³

Shell-model calculations fitting the properties of low-lying states in the mass region 29-40 have been performed by Glaudemans, Wiechers, and Brussaard.²¹ These authors assumed an inert ${}^{28}\text{Si}$ core and considered only excitations in the $2s_{1/2}$ and $1d_{3/2}$ shells. More recent shell-model calculations²² include additional states with up to two holes in the $1d_{5/2}$ shell. With these wave functions, Glaudemans, Endt, and Dieperink²³ have calculated electromagnetic transition rates in $A=30-34$ nuclei. The calculations for $M1$ transitions were performed with (i) bare-nucleon g factors, (ii) "effective" g factors determined from a least-squares fit to many $M1$ transition rates measured in this mass region, and (iii) "effective" single-particle matrix elements also obtained from a fit to experimental data. The stronger $M1$ transitions observed experimentally throughout the s - d shell are well fitted by all three methods. The best fit is found by using the effective matrix elements, and the calculations with these predict

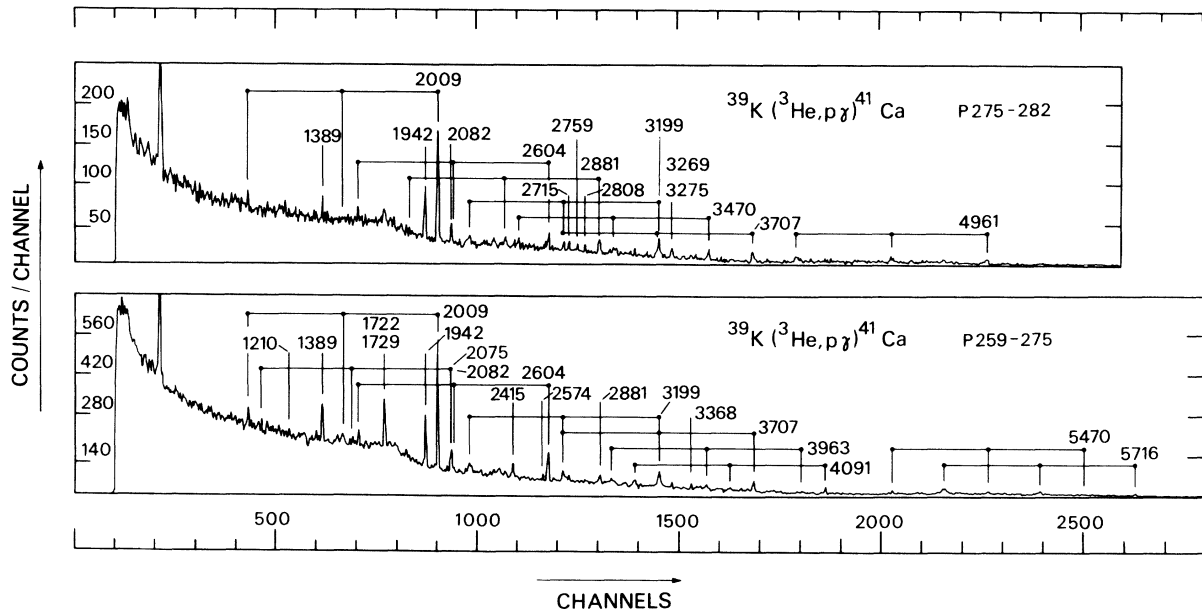


FIG. 11. Coincidence spectra as in Fig. 9, except that the ranges of channel numbers are 275-282 (upper spectrum) and 259-275 (lower spectrum). The energies $E_\gamma = E_x^i - E_x^f$ (keV) for the peaks are 1210=4091-2881, 1389=3398-2009, 1722=5813 (isobaric analog state)-4091, 1729=3738-2009, 1942=1942-g.s., 2009=2009-g.s., 2075=5813 (isobaric analog state)-3738, 2082=4091-2009, 2415=5813 (isobaric analog state)-3398, 2574=2574-g.s., 2604=2604-g.s., 2715=4724-2009, 2759=4768-2009, 2808=5412-2604, 2881=2881-g.s., 3199=3199-g.s., 3269=5211-1942, 3275=5284-2009, 3368=5972-2604, 3470=5412-1942, 3707=5716-2009, 3963=5972-2009, 4091=4091-g.s., 4961=4961-g.s., 5470=5470-g.s., 5716=5716-g.s.

relative intensities of 89% and 11% for the transitions from the analog state in ^{33}S to the first excited state and to the ground state, respectively. These values are in good agreement with the values 85% and 15% measured here.

The γ decay from the analog state to the 842-keV level is thus presumably a strong $M1$ transition. The relative intensity of the transition to the ground state is therefore perhaps somewhat surprising – at least if one considers only a simple model in which the ground state of ^{33}S would have the principal configuration

$$[s_{1/2}^4(0,0)d_{3/2}^1(\frac{1}{2}, \frac{1}{2})]_{(3/2, 1/2)},$$

since this configuration would not permit an $M1$ transition. The assumed simple configurations

for the 5479-keV analog state and for the ground state would permit an $E2$ transition between them. Possibly the observed transition does contain a large $E2$ component, although it would be somewhat surprising to find an $E2$ transition with an intensity comparable to that of the strong $M1$ to the 842-keV level. The more complete shell-model calculations^{22, 23} show that the wave functions for most of the low-lying even-parity states in ^{33}S contain quite large admixtures of other configurations (e.g., configurations in which additional particles are raised out of the $2s_{1/2}$ and $1d_{5/2}$ shells). It is likely that through such additional components the ground-state γ -ray transition from the analog state obtains its relatively high transition probability. It is interesting to note that the

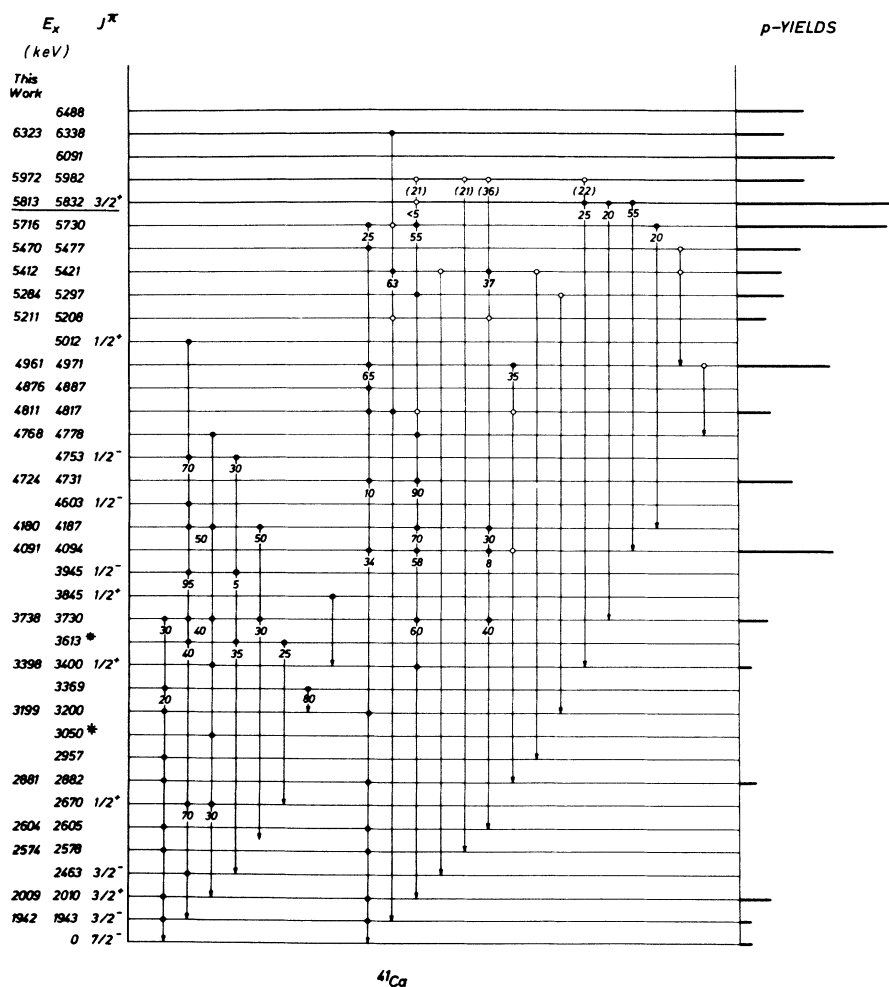


FIG. 12. γ -decay scheme for ^{41}Ca . The notation and conventions used are the same as for Fig. 7. The left-hand column of excitation energies lists values determined from the present work (i.e., from the γ spectra) and the other column of energies gives the values from Refs. 6 and 12. For the states marked with an asterisk, Ref. 6 gives the following branches: 3050-keV level: 10% to the ground state, 35% to the first or second excited state, and 55% to the state at 2605 or 2578 keV; 3613-keV level: 25% to the ground state, 44% to the first or second excited state, and 31% to the 2463-keV state.

γ decay of the corresponding analog state in ^{33}Cl proceeds >90% via the $\frac{1}{2}^+$, $T = \frac{1}{2}$ state at 806 keV and that the ground-state transition represents less than 10% of the γ decay.²⁴

Using the known^{12, 25} properties of low-lying states in ^{33}P , one can predict that in ^{33}S the lowest $T = \frac{3}{2}$ states (in addition to the 5475-keV level) are to be expected at energies of approximately 6900, 7320, and 8000 keV with spins of $\frac{3}{2}^+$, $\frac{5}{2}^+$, and $\frac{3}{2}^+$, respectively. Transitions to the three corresponding levels in ^{33}P are seen²⁵ as $L = 2$ transfers in the $^{31}\text{P}(t, p)^{33}\text{P}$ reaction. In the (t, p) reaction, however, these transitions are weak (a few per cent) relative to the strong $L = 0$ transition to the $\frac{1}{2}^+$, $T = \frac{3}{2}$ ground state of ^{33}P . In the present work (as seen in Table I) there are several transitions that could correspond to those seen in the (t, p) reaction. Definite assignments are, however, not possible. There is evidence for a very strong transition in the $(^3\text{He}, p)$ reaction to a level at 7920 keV which γ -decays to the 842-keV level. Unfortunately, no proton angular distribution could be measured for the 7920-keV level; but its strength and the fact that a γ decay is measurable, even though the threshold for α emission from ^{33}S is at 7114 keV, both suggest a $T = \frac{3}{2}$ assignment.

In ^{41}Ca , the absence of a γ -ray transition from the lowest analog state to the 2010-keV state is a striking feature. Information on the structure of the low-lying positive-parity states in ^{41}Ca is available from reaction data, including the $^{39}\text{K}(^3\text{He}, p)^{41}\text{Ca}$ measurements of Belote *et al.*¹⁵ and of Seth *et al.*,²⁶ and also from the shell-model calculations of Sartoris and Zamick²⁷ and of Lawson.²⁸ The $(^3\text{He}, p)$ measurements show several strong transitions whose angular distributions are peaked in the forward direction. The most intense of these transitions (which are presumed to involve the transfer of $L = 0$ neutron-proton pairs) are to the ^{41}Ca states whose excitation energies (keV), followed in parentheses by the differential cross sections (mb/sr) measured at $\theta_p = 7.5^\circ$ by Belote *et al.*,¹⁵ are 2010 (0.19), 3400 (0.07), 3730 (0.18), 4094 (0.51), 4731 (0.30), 4817 (0.17), 5832 (0.91), and 5982 (0.38).

In the simplest shell-model description of ^{41}Ca , one would expect the analog state at 5832 keV to have mainly the configuration

$$[d_{3/2}^{-1}(\frac{3}{2}, \frac{1}{2})f_{7/2}^2(0, 1)]_{(3/2, 3/2)}.$$

Similarly, the 2010-keV level would be mainly $[d_{3/2}^{-1}(\frac{3}{2}, \frac{1}{2})f_{7/2}^2(0, 1)]_{(3/2, 1/2)}$ with perhaps also a contribution from $[d_{3/2}^{-1}(\frac{3}{2}, \frac{1}{2})f_{7/2}^2(1, 0)]_{(3/2, 1/2)}$. [In ^{42}Sc , the $f_{7/2}(1, 0)$ configuration lies 0.62 MeV above the $f_{7/2}^2(0, 1)$ configuration.] One would also expect three states at low excitation energies with principal configurations of the type

$$[d_{3/2}^{-1}(\frac{3}{2}, \frac{1}{2})f_{7/2}^2(1, 0)]$$

with $T = \frac{1}{2}$ and spins $\frac{1}{2}^+$, $\frac{3}{2}^+$, and $\frac{5}{2}^+$. Additional possible components containing other couplings of the two $f_{7/2}$ particles would be expected to be small. All of these states should be populated strongly in the $^{39}\text{K}(^3\text{He}, p)^{41}\text{Ca}$ reaction and weakly in the $^{40}\text{Ca}(d, p)^{41}\text{Ca}$ reaction. In the neutron-pickup reactions on a ^{42}Ca target, the states with large $(f_{7/2}^2)_{0,1}$ components should show up strongly and those with $(f_{7/2}^2)_{1,0}$ only weakly.

In their shell-model calculations of the low-lying positive-parity levels of ^{41}Ca , Sartoris and Zamick²⁷ and Lawson²⁸ took account of configurations consisting of a single hole in the s - d shell and two valence nucleons in the $2p$ - $1f$ shell. Their calculations produce levels having the principal configurations listed above, but the fits to the known energies in ^{41}Ca are poor and therefore they made no attempt to calculate transition probabilities between these levels. Both sets of calculations produce predominantly

$$[d_{3/2}^{-1}(\frac{3}{2}, \frac{1}{2})f_{7/2}^2(0, 1)]$$

configurations for the lowest $J = \frac{3}{2}^+$, $T = \frac{1}{2}$ state and for the lowest $J = \frac{3}{2}^+$, $T = \frac{3}{2}$ state. This, together with the experimental evidence on stripping and pickup reactions, strongly suggests that the 2010-keV level in ^{41}Ca is the most likely candidate for the $T <$ state corresponding to the 5832-keV $\frac{3}{2}^+$, $T = \frac{3}{2}$ analog state. [Both states are only weakly excited²⁹ in the $^{40}\text{Ca}(d, p)^{41}\text{Ca}$ reaction but are strongly populated in the $^{39}\text{K}(^3\text{He}, p)^{41}\text{Ca}$ reaction and in neutron-pickup reactions³⁰⁻³² on ^{42}Ca .] The question then arises as to why the expected $M1$ transition between these two levels was not observed, while in ^{33}S the corresponding transition was quite strong. The answer to this may lie in the following considerations.

Maripuu¹⁸ has calculated $M1$ transition probabilities between states formed by a single nucleon in an orbit (l, j) coupled to a core having $J = 0$ and isospin T . That is, $M1$ transitions between states $(J = j, T + \frac{1}{2})$ and $(J = j, T - \frac{1}{2})$ are considered. Maripuu points out that the isovector part of the $M1$ transition probability then contains the factor $(g_p - g_n)^2$, where g_p and g_n are the gyromagnetic ratios of the proton and neutron, respectively, in the orbit (l, j) . Consequently, $M1$ isovector matrix elements between states with $j = l + \frac{1}{2}$ are much larger than those between states with $j = l - \frac{1}{2}$. (In the "parallel" case, the orbital and spin-projected magnetic moments of the proton and the spin-projected magnetic moment of the neutron all add up to give a maximum in the quantity $|g_p - g_n|$. In the "antiparallel" case, a minimum in $|g_p - g_n|$ results.) Thus, for example, the single-particle $M1$

transition probability between members of an isospin doublet with $T_> = \frac{3}{2}$ and $T_< = \frac{1}{2}$ for a $d_{5/2}$ nucleon is 1.85 Weisskopf units (W.u.), whereas the corresponding value for a $d_{3/2}$ nucleon is only 0.051 W.u. – about a factor of 40 smaller. The corresponding value for an $s_{1/2}$ nucleon is 1.95 W.u., and for an $f_{7/2}$ nucleon it is 2.24 W.u. These results help to explain why experimentally observed $M1$ transitions between $d_{3/2}^N$ configurations are so weak¹⁹ (on the order of 0.01 W.u.).

One can apply these ideas to the γ decays of the lowest analog states in ^{33}S and ^{41}Ca by considering these states and their corresponding $T_<$ states as consisting of a single $s_{1/2}$ hole (^{33}S) or a single $d_{3/2}$ hole (^{41}Ca) coupled to $J=0, T=1$ cores of ^{34}S and ^{42}Ca , respectively. Thus the strong $M1$ transition observed in ^{33}S between the 5479- and 842-keV states would be explained as being an example of a favored ($j = l + \frac{1}{2}$) transition involving an $s_{1/2}$ hole. The absence of an observed transition between the 5832-keV and the 2010-keV states in ^{42}Ca would be explained as being a case of an inhibited ($j = l - \frac{1}{2}$) transition involving a $d_{3/2}$ hole.

In addition to the contributions of the single holes to the $M1$ transitions under consideration, there may also be contributions arising from rearrangements of the core nucleons. For example, in ^{33}S the 842-keV level could contain an admixture of the configuration $[s_{1/2}^{-1}(\frac{1}{2}, \frac{1}{2})d_{3/2}^2(1, 0)]_{(1/2, 1/2)}$. This would then permit an $M1$ transition between the $d_{3/2}^2(0, 1)$ core configuration of the analog state and the $d_{3/2}^2(1, 0)$ component of the core configuration for the 842-keV state. However, since such a transition would involve a $d_{3/2}$ nucleon, one would expect its contribution to be small. Similar considerations apply to the $f_{7/2}$ core nucleons in the ^{41}Ca case, except that now one would expect their contributions to be strong. The absence of an observed transition between the 5832- and 2010-keV states in ^{41}Ca can thus be taken as evidence that the 2010-keV level contains very little of the configuration

$$[d_{3/2}^{-1}(\frac{3}{2}, \frac{1}{2})f_{7/2}^2(1, 0)]_{(3/2, 1/2)}.$$

Shell-model calculations^{27, 28} also yield very little of this configuration in the lowest $J = \frac{3}{2}^+, T = \frac{1}{2}$ state calculated for ^{41}Ca .

In both ^{33}S and ^{41}Ca , one would expect low-lying states of positive parity in which the two outermost core nucleons couple to $J=1$ and $T=0$. Thus in ^{33}S , one expects two states with principal configurations $[s_{1/2}^{-1}(\frac{1}{2}, \frac{1}{2})d_{3/2}^2(1, 0)]_{(1/2 \text{ or } 3/2, T=1/2)}$ lying 1–2 MeV above the 842-keV state; and similarly in ^{41}Ca , three states with mainly

$$[d_{3/2}^{-1}(\frac{1}{2}, \frac{1}{2})f_{7/2}^2(1, 0)]_{(1/2, 3/2, \text{ or } 5/2, T=1/2)}$$

are expected a little above the 2010-keV state. Such states would be populated fairly strongly in the $(^3\text{He}, p)$ reaction with the $L=0$ transfer of a $J=1, T=0$ neutron-proton pair and should appear only weakly, if at all, in the neutron-pickup reactions on targets of ^{34}S and ^{42}Ca . States meeting these requirements are observed at excitation energies of 4068, 4389, and 4761 keV in ^{33}S and at 3400, 3730, 4094, 4731, and 4817 keV in ^{41}Ca . It is interesting to note that whereas the $(^3\text{He}, p)$ transitions involving the presumed $L=0$ transfer of a $J=0, T=1$ neutron-proton pair to the analog states and their corresponding $T_<$ states display quite deep minima at about 30° in their angular distributions, this feature is missing in the angular distributions for some of the levels mentioned above (specifically, for the 4068-, 4389-, and 4761-keV levels in ^{33}S and for the 3400-, 3730-, and 4094-keV levels in ^{42}Ca). This “filling in” of angular distributions at about 30° is a characteristic that has been observed in other $(^3\text{He}, p)$ work³³ and has been used to distinguish between transitions leading from a 0^+ initial state to final states of either 0^+ or 1^+ . It has been suggested³³ that this feature may be due to $L=2$ contributions in the case of a 1^+ final state. However, the results of the present work on the $^{39}\text{K}(^3\text{He}, p\gamma)^{41}\text{Ca}$ reaction suggest the possibility that the “filling in” may be simply a consequence of the fact that a $J=1, T=0$

TABLE II. A comparison of the relative reduced transition probabilities for γ decays from the 5832-keV analog state to the levels at 4094, 3730, and 3400 keV in ^{41}Ca , with the relative differential cross sections (Ref. 15) for the population of these levels in the $^{39}\text{K}(^3\text{He}, p)^{41}\text{Ca}$ reaction.

| Excitation energy (keV) | J^π | γ branching | | Relative reduced γ -ray transition probability | $d\sigma/d\Omega(7.5^\circ)$ $^{39}\text{K}(^3\text{He}, p)^{41}\text{Ca}$ (mb/sr) | Relative $d\sigma/d\Omega(7.5^\circ)$ $^{39}\text{K}(^3\text{He}, p)^{41}\text{Ca}$ | |
|-------------------------|---------------------------------|-------------------------------|------|---|--|--|--|
| | | ratio from 5832-keV state (%) | | | | Ratio Col. 6/Col. 4 | |
| 4094 | $\frac{5}{2}^+$ | 55 | 6 | 0.51 | 6 | 1.0 | |
| 3730 | Spin unknown positive parity | 20 | 1.25 | 0.18 | 2.1 | 1.7 | |
| 3400 | $\frac{1}{2}^+$ | 25 | 1.0 | 0.07 | 0.82 | 0.8 | |

neutron pair is being transferred and it may be present even in the case of a pure $L=0$ transfer.

The 3400-keV level in ^{41}Ca is known¹² to be $\frac{1}{2}^+$. The 4094-keV level in ^{41}Ca was previously known¹² to have positive parity and to have a spin of either $\frac{1}{2}$, $\frac{3}{2}$, or $\frac{5}{2}$. From the present observation of a strong γ -ray branch (34%) to the $\frac{7}{2}^-$ ground state, it can reasonably be assumed³⁴ that the transition is predominantly $E1$ and that therefore the 4094-keV state has $J^\pi = \frac{5}{2}^+$.

The fact that the γ decay from the 5832-keV analog state proceeds to the levels at 4094 keV (55%), 3730 keV (20%), and 3400 keV (24%) is further evidence that these levels have predominantly $[d_{3/2}^{-1}(\frac{1}{2}, \frac{1}{2})f_{7/2}^2(1,0)]$ configurations. The γ decays would then be explained as being the strong $M1$ transitions expected between the $f_{7/2}^2(0,1)$ core component of the analog state and the $f_{7/2}^2(1,0)$ components of the 4094-, 3730-, and 3400-keV states.

It has been pointed out³⁵ that if the ^{41}Ca states under consideration here have predominantly the configurations that have been discussed above, then the branching ratios for γ decay from the 5832-keV analog state to the states at 4094, 3730, and 3400 keV should have some simple relation to the relative cross sections with which these states are populated in the $(^3\text{He}, p)$ reaction. The reduced γ -ray transition probabilities to these states should be proportional to

$$(2J_f + 1)[C_{d_{3/2}^{-1}(\frac{1}{2}, \frac{1}{2})}^{J_f, 1/2}]^2,$$

where J_f is the spin of the final state and the coefficient $C_{d_{3/2}^{-1}(\frac{1}{2}, \frac{1}{2})}^{J_f, 1/2}$ is a measure of the amount of the configuration $[d_{3/2}^{-1}(\frac{3}{2}, \frac{1}{2})f_{7/2}^2(1,0)]_{(J_f, 1/2)}$ contributing to the wave functions of the final states. The cross section $d\sigma/d\Omega$ for the $(^3\text{He}, p)$ reaction to these same final states should also be proportional to $(2J_f + 1)[C_{d_{3/2}^{-1}(\frac{1}{2}, \frac{1}{2})}^{J_f, 1/2}]^2$ under the assumption that the contribution from the configuration $[d_{3/2}^{-1}(\frac{3}{2}, \frac{1}{2})f_{7/2}^2(0,1)]_{(3/2, 1/2)}$ is small for the $J = \frac{3}{2}, T = \frac{1}{2}$ state. (The spin of the 3730-keV level in ^{41}Ca has not yet been measured. It would be interesting to determine whether this level does indeed have spin and parity $\frac{3}{2}^+$.) Table II compares these quantities. The reasonably good agreement between the relative γ -transition rates and the cross sections for the $(^3\text{He}, p)$ reaction is additional evidence that the structure of these levels is being correctly interpreted.

The γ decays of the three levels at 4094, 3730, and 3400 keV in ^{41}Ca proceeds predominantly to the 2010-keV level. This again is consistent with the postulated structure of the levels involved. These γ decays can then be easily explained as being the expected strong $M1$ transitions between the predominant $f_{7/2}^2(1,0)$ configurations present in the upper three levels and the $f_{7/2}^2(0,1)$, which is expected to dominate in the wave function for the 2010-keV level.

Since the γ transition from the 4094–2010-keV level is expected to be a strong and fairly pure $M1$, it is perhaps a little surprising that there exists a competitive transition (34%) to the $\frac{7}{2}^-$ ground state of ^{41}Ca . Such an $E1$ transition would be highly unlikely if the configurations of the 4094-keV state and the ground state were of the simple type described above. It has been shown,³⁵ however, that an admixture to the wave function of the 4094-keV level of only 2% in intensity of the configuration $[d_{5/2}^{-1}(\frac{5}{2}, \frac{1}{2})f_{7/2}^2(0,1)]_{(5/2, 1/2)}$ would account for the relative strength of the observed γ transition to the ground state. This transition would then be an $E1$ resulting from the filling of the $d_{5/2}$ hole by one of the $f_{7/2}$ nucleons. Further evidence for the existence of a $d_{5/2}$ hole component in the 4094-keV state is found in the observations³⁰ on the pickup reaction $^{42}\text{Ca}(p, d)^{41}\text{Ca}$, in which this state is seen with a small but observable intensity as an $l_n = 2$ transition. In measurements on the $^{42}\text{Ca}(^3\text{He}, \alpha)^{41}\text{Ca}$ reaction³² the transition to the 4094-keV state was assigned $l_n = 3$. It would seem likely that the difficulties in distinguishing between $l_n = 2$ and $l_n = 3$ angular distributions in the $(^3\text{He}, \alpha)$ reactions (especially for weak transitions) has led to an incorrect assignment in this case, since an $l_n = 3$ transfer in the $(^3\text{He}, \alpha)$ reaction would be very difficult to reconcile with all of the other measurements on the 4094-keV level.

ACKNOWLEDGMENTS

We wish to thank Dr. W. Gentner for making available to us the accelerators and associated facilities at the Max-Planck-Institut für Kernphysik, Heidelberg, Germany, where a large fraction of the work reported here was performed. We also gratefully acknowledge several stimulating discussions with Dr. D. Kurath and Dr. R. D. Lawson.

*Part of this work was done at the Max-Planck-Institut für Kernphysik, Heidelberg, Germany, while this author was visiting there for one year.

†Present address: Institute for Nuclear Study, Tokyo University, Tanashi, Tokyo, Japan.

‡Present address: Physics Department, Bangalore

University, Mysore State, Bangalore, India.

¹P. M. Endt, in *Proceedings of the Conference on Nuclear Isospin, Asilomar-Pacific Grove, California, March, 1969*, edited by J. D. Anderson, S. D. Bloom, J. Cerny, and W. W. True (Academic Press Inc., New York, 1969).

²S. S. Hanna, in *Isospin in Nuclear Physics*, edited by D. H. Wilkinson (North-Holland Publishing Company, Amsterdam, The Netherlands, 1969).

³F. C. Ern e, W. A. M. Veltmann, and J. A. J. M. Wintermans, Nucl. Phys. 88, 1 (1966).

⁴L. Meyer-Sch utzmeister, D. S. Gemmell, R. E. Holland, F. T. Kuchnir, H. Ohnuma, and N. G. Puttaswamy, Phys. Rev. 187, 1210 (1969).

⁵J. A. Spencer and H. A. Enge, Nucl. Instr. Methods 49, 181 (1967).

⁶J. R. Erskine and R. H. Vonderohe, Nucl. Instr. Methods 81, 221 (1970).

⁷D. S. Gemmell, Nucl. Instr. Methods 46, 1 (1966).

⁸Purchased from SIMTEC, Montreal, Canada.

⁹S. Kalbitzer, R. Bader, H. Herzer, and K. Bethge, Z. Physik 203, 117 (1967).

¹⁰Purchased from ORTEC, Oak Ridge, Tennessee, U. S. A.

¹¹J. Fr uh, Ph.D. thesis, Stuttgart University, Stuttgart, Germany, 1969 (unpublished).

¹²P. M. Endt and C. Van der Leun, Nucl. Phys. A105, 1 (1967).

¹³R. S. Cox, R. W. West, and R. J. Ascutto, Phys. Rev. 175, 1419 (1968).

¹⁴J. Dubois, Nucl. Phys. A117, 533 (1968).

¹⁵T. A. Belote, F. T. Dao, W. E. Dorenbusch, J. Kuperus, and J. Rappaport, Phys. Letters 23, 480 (1966); T. A. Belote, F. T. Dao, W. E. Dorenbusch, K. Kuperus, J. Rappaport, and S. M. Smith, Nucl. Phys. A102, 462 (1967).

¹⁶G. Johnson, R. S. Blake, H. Laurent, F. Picard, and J. P. Schapira, Nucl. Phys. A143, 562 (1970).

¹⁷H. Gruppelaar and P. Spilling, Nucl. Phys. A102, 226 (1967).

¹⁸S. Maripuu, Nucl. Phys. A123, 357 (1969).

¹⁹D. Kurath, Bull. Am. Phys. Soc. 13, 1400 (1968); Argonne National Laboratory Report No. ANL-7512, 1968 (unpublished), p.84.

²⁰J. R. Erskine, D. J. Crozier, J. P. Schiffer, and W. P. Alford, to be published.

²¹P. W. M. Glaudemans, G. Wiechers, and P. J. Brussaard, Nucl. Phys. 56, 548 (1964).

²²B. H. Wildenthal, J. B. McGrory, E. C. Halbert, and P. W. M. Glaudemans, Phys. Letters 27B, 611 (1968).

²³P. W. M. Glaudemans, P. M. Endt, and A. E. L. Dieperink, to be published.

²⁴L. M. Spitz and F. D. Brooks, in *Proceedings of the International Conference on Properties of Nuclear States, Montr eal, Canada, 1969*, edited by M. Harvey *et al.* (Les Presses de l'Universit e de Montr eal, Montr eal, Canada, 1969), p. 765; and private communication.

²⁵W. G. Davies, J. C. Hardy, and W. Darcey, Nucl. Phys. A128, 465 (1969).

²⁶K. K. Seth, R. G. Couch, J. A. Biggerstaff, and P. D. Miller, Phys. Rev. Letters 17, 1294 (1966).

²⁷G. Sartoris and L. Zamick, Phys. Rev. Letters 18, 292 (1967).

²⁸R. D. Lawson, private communication.

²⁹T. A. Belote, A. Sperduto, and W. W. Buechner, Phys. Rev. 139, B80 (1965).

³⁰S. M. Smith, A. M. Bernstein, and M. E. Rickey, Nucl. Phys. A113, 303 (1968).

³¹R. Bock, H. H. Duhm, and R. Stock, Phys. Letters 18, 61 (1965).

³²U. Lynen, R. Bock, R. Santo, and R. Stock, Phys. Letters 25B, 9 (1967).

³³O. Hansen, in *Proceedings of the International Conference on Properties of Nuclear States, Montr eal, Canada, 1969*, edited by M. Harvey *et al.* (Les Presses de l'Universit e de Montr eal, Montr eal, Canada, 1969), p. 421.

³⁴D. S. Gemmell, L. Meyer-Sch utzmeister, H. Ohnuma, and N. G. Puttaswamy, Bull. Am. Phys. Soc. 12, 1183 (1967).

³⁵D. Kurath, private communication.